Journal of Organometallic Chemistry, 267 (1984) 237–247
Elsevier Sequoia S.A., Lausanne – Printed in The Netherlands

ORGANOTIN BIOCIDES

I. THE STRUCTURE OF TRIPHENYLTIN ACETATE

K.C. MOLLOY *, T.G. PURCELL, K. QUILL,
School of Chemical Sciences, National Institute for Higher Education, Glasnevin, Dublin 9 (Ireland)

and I.W. NOWELL
Department of Chemistry, Sheffield City Polytechnic, Pond Street, Sheffield S1 1WB (Great Britain)

(Received January 16th, 1984)

Summary

The crystal structure of triphenyltin acetate has been determined using heavy atom methods in conjunction with least squares refinement of data measured on a two-circle diffractometer. Crystals are monoclinic, space group $P2_1/c$, cell dimensions a 8.969(4), b 10.146(5), c 19.540(7) Å, β 93.70(4)°, $U = 1774.5$ Å^3 and $Z = 4$. The structure was refined using 1841 observed reflections to give conventional discrepancy factors of $R = 0.022$ and $R' = 0.023$. The environment at tin is described in terms of a distorted, six-coordinate, *mer*-Ph_3SnO_3 geometry, the first six-coordinate triorganotin structure authenticated crystallographically. Carboxylate bridges link subunits together to form a flattened helical polymer. Variable temperature Mössbauer spectroscopy ($a = \mathrm{d}\ln A(T)/\mathrm{d}T = -1.91 \times 10^{-2}$ K^{-1}) suggests that polymers of this type afford tin atoms the same vibrational freedom normally associated with non-interacting lattices.

Introduction

Organotin compounds are extensively used as biocides, with some 10,000 tonnes of these compounds currently in use [1]. This commercialisation reflects both the versatility of this class with respect to a variety of biocidal fields (agrochemicals, surface disinfectants, wood preservatives, marine anti-fouling paints [2]) and a favourable environment degradation pathway to non-toxic inorganic tin. This latter property in particular sets organotins apart from similarly used organoarsenic and

---

* Address for correspondence

0022-328X/84/$03.00

organomercury compounds, whose environmental fate is less desirable due to the ease with which these elements are biomethylated to volatile, highly toxic methylmetals [3].

Triphenyltin acetate has itself been used since the early 1960's (Brestan®, Hoechst A.G.) to control potato blight (*Phytophthora infestans*), and is as effective against a range of fungi as conventional copper-based formulations but at one-tenth the dose [4]. We initiate this series of studies into the synthetic and structural chemistry of organotins with known or potential biocidal properties by reporting the structure of this important agrochemical, as studied by both single crystal X-ray diffraction and variable temperature Mössbauer spectroscopy.

Experimental

Recrystallisation of the product of the reaction between triphenyltin hydroxide and the betaine $(HOOCCH_2\overset{+}{N}C_5H_4C_5H_4\overset{+}{N}CH_2COOH) \cdot 2Cl^-$ from acetic acid/methanol (20/80) yielded triphenyltin acetate as the only identifiable product [5]. Further recrystallisation from the same solvent mixture afforded crystals suitable for X-ray study. The sample of $Ph_3SnO_2CCH_3$ used in the Mössbauer study was prepared by literature methods [6], and found to be analytically pure *. The melting point of a mixture of products from the two sources showed no depression.

Mössbauer Data

Mössbauer spectra were recorded on a constant acceleration Mössbauer spectrometer (Cryophysics) fitted with a room temperature 5 mCi calcium stannate-119m source (Amersham Int.) and operated in a sawtooth wave mode. Temperature control of the sample was achieved using a continuous flow, liquid nitrogen cryostat linked to a DTC-2 digital variable temperature controller (Oxford Instruments). Temperature stability was ± 0.1 K of the desired temperature throughout spectral accumulation. Samples were prepared as finely ground powders to avoid orientation effects. Velocity calibration was based on the spectrum of natural iron, and $CaSnO_3$ used as the zero velocity reference. Spectra were curve fitted using conventional least-squares techniques to standard Lorentzian line shapes, with prior data correction for parabolic background curvature.

Crystal data

$C_{20}H_{18}O_2Sn$, $M = 409.1$, monoclinic $P2_1/c$, a 8.969(4), b 10.146(5), c 19.540(7) Å, β 93.70(4)°, U 1774.5 Å^3, $Z = 4$, D_c 1.53, D_m 1.51 $Mg m^{-3}$, $\mu(\text{Mo-}K_\alpha)$ 1.32 mm^{-1}, $F(000) = 816$.

Data collection and reduction

A crystal of approximate dimensions $0.13 \times 0.14 \times 0.35$ mm was used for data collection and was mounted with the b axis coincident with the rotation (ω) axis of a Stöe Stadi-2 two circle diffractometer. 2163 unique reflection were collected, of which 1841 had $I \geqslant 3\sigma(I)$ and were considered as observed and used for subsequent

---

* Found: C, 58.34; H, 4.39. $C_{20}H_{18}O_2Sn$ calcd.: C, 58.72; H, 4.44%.

analysis. Corrections were made for Lorentz and polarisation effects, but no corrections were applied for absorption.

Structure determination and refinement

The approximate position of the tin atom was calculated using a three-dimensional Patterson synthesis. The remaining atoms were located from successive difference Fourier maps. The hydrogen atoms were located, but given ideal geometry

TABLE 1

FRACTIONAL POSITIONAL PARAMETERS ($\times 10^5$ for Sn; $\times 10^4$ for remaining atoms) WITH e.s.d.'s FOR NON-HYDROGEN ATOMS IN PARENTHESES

Atom	*x*	*y*	*z*
Sn	91578(3)	30183(2)	76237(1)
O(1)	9523(3)	−121(3)	7720(1)
O(2)	7950(3)	1382(3)	8060(1)
C(1)	8492(5)	232(4)	8081(2)
C(2)	7846(6)	−680(4)	8587(2)
C(11)	7618(4)	4343(3)	8033(2)
C(12)	6277(5)	4651(5)	7673(2)
C(13)	5274(5)	5527(6)	7936(3)
C(14)	5568(5)	6079(5)	8572(3)
C(15)	6887(5)	5795(4)	8931(2)
C(16)	7905(5)	4944(4)	8666(2)
C(21)	11045(4)	2613(4)	8316(2)
C(22)	10748(5)	2353(4)	8996(2)
C(23)	11906(7)	2123(4)	9485(2)
C(24)	13357(7)	2147(5)	9318(3)
C(25)	13672(6)	2393(6)	8661(3)
C(26)	12516(5)	2631(5)	8154(3)
C(31)	8578(4)	2616(4)	6569(2)
C(32)	8471(5)	1356(4)	6299(2)
C(33)	7983(5)	1159(5)	5617(2)
C(34)	7553(5)	2202(5)	5202(2)
C(35)	7635(6)	3455(5)	5467(2)
C(36)	8141(5)	3663(5)	6145(2)
H(111)	8394	−1625	8563
H(112)	6664	−800	8462
H(113)	8022	−281	9098
H(12)	6014	4192	7182
H(13)	4259	5786	7639
H(14)	4760	6719	8790
H(15)	7140	6243	9426
H(16)	8953	4742	8950
H(22)	9601	2331	9134
H(23)	11652	1931	10008
H(24)	14247	1960	9705
H(25)	14819	2410	8523
H(26)	12766	2831	7630
H(32)	8766	526	6627
H(33)	7937	171	5411
H(34)	7164	2038	4674
H(35)	7303	4285	5146
H(36)	8200	4650	6352

(C–H 1.08 Å). Scattering factors were calculated using an analytical approximation [7] and the weighting scheme adopted was $w = 1.2022/[\sigma^2(F_o) + 0.003(F_o)^2]$. The phenyl and methyl hydrogen atoms were given common isotropic temperature factors which refined to final values of $U = 0.091(5)$, $0.177(17)$ Å^2. All other atoms were given anisotropic temperature factors and full matrix least-squares refinement gave final values of $R = 0.022$ and $R' = 0.023$. The final positional parameters are given in Table 1, bond distances and angles in Table 2. The coordination about tin

TABLE 2

BOND DISTANCES (Å) AND ANGLES (°) WITH e.s.d.'s IN PARENTHESES. SYMMETRY CODE NONE x, y, z, (′) $2-x, 0.5+y, 1.5-z$; (″) $2-x, -0.5+y, 1.5-z$

Bond distances			
Sn–O(1)	3.206(3)	C(16)–C(11)	1.388(5)
Sn–O(1′)	2.349(3)	C(21)–C(22)	1.397(6)
Sn–O(2)	2.185(3)	C(22)–C(23)	1.385(7)
Sn–C(11)	2.120(4)	C(23)–C(24)	1.362(8)
Sn–C(21)	2.138(4)	C(24)–C(25)	1.356(9)
Sn–C(31)	2.133(4)	C(25)–C(26)	1.408(7)
O(1)–C(1)	1.251(5)	C(26)–C(21)	1.377(6)
O(2)–C(1)	1.263(5)	C(31)–C(32)	1.384(6)
C(1)–C(2)	1.497(6)	C(32)–C(33)	1.391(6)
C(11)–C(12)	1.390(6)	C(33)–C(34)	1.374(6)
C(12)–C(13)	1.387(7)	C(34)–C(35)	1.372(7)
C(13)–C(14)	1.373(8)	C(35)–C(36)	1.389(6)
C(14)–C(15)	1.366(7)	C(36)–C(31)	1.387(6)
C(15)–C(16)	1.381(6)		
Bond angles			
O(1)–Sn–O(1′)	139.8(1)	Sn–C(11)–C(12)	121.0(3)
O(1)–Sn–O(2)	43.4(1)	Sn–C(11)–C(16)	121.8(3)
O(1)–Sn–C(11)	132.4(1)	C(12)–C(11)–C(16)	117.2(4)
O(1)–Sn–C(21)	72.4(1)	C(11)–C(12)–C(13)	121.2(4)
O(1)–Sn–C(31)	83.4(1)	C(12)–C(13)–C(14)	120.3(4)
O(1′)–Sn–O(2)	173.6(1)	C(13)–C(14)–C(15)	119.2(5)
O(1′)–Sn–C(11)	87.2(1)	C(14)–C(15)–C(16)	120.7(4)
O(1′)–Sn–C(21)	86.7(1)	C(11)–C(16)–C(15)	121.3(4)
O(1′)–Sn–C(31)	88.5(1)	Sn–C(21)–C(22)	116.5(3)
O(2)–Sn–C(11)	89.0(1)	Sn–C(21)–C(26)	125.6(3)
O(2)–Sn–C(21)	90.0(1)	C(22)–C(21)–C(26)	117.8(4)
O(2)–Sn–C(31)	97.8(1)	C(21)–C(22)–C(23)	120.5(4)
C(11)–Sn–C(21)	113.0(1)	C(22)–C(23)–C(24)	121.2(5)
C(11)–Sn–C(31)	111.2(1)	C(23)–C(24)–C(25)	119.4(5)
C(21)–Sn–C(31)	135.2(1)	C(24)–C(25)–C(26)	120.6(5)
Sn–O(1)–Sn″	146.4(1)	C(21)–C(26)–C(25)	120.6(5)
Sn–O(1)–C(1)	70.9(1)	Sn–C(31)–C(32)	123.4(3)
Sn″–O(1)–C(1)	142.7(2)	Sn–C(31)–C(36)	118.1(3)
Sn–O(2)–C(1)	121.0(2)	C(32)–C(31)–C(36)	118.1(3)
O(1)–C(1)–O(2)	122.9(4)	C(31)–C(32)–C(33)	120.5(4)
O(1)–C(1)–C(2)	121.8(4)	C(32)–C(33)–C(34)	120.9(4)
O(2)–C(1)–C(2)	115.3(4)	C(33)–C(34)–C(35)	119.0(4)
		C(34)–C(35)–C(36)	120.5(4)
		C(31)–C(36)–C(35)	121.0(4)

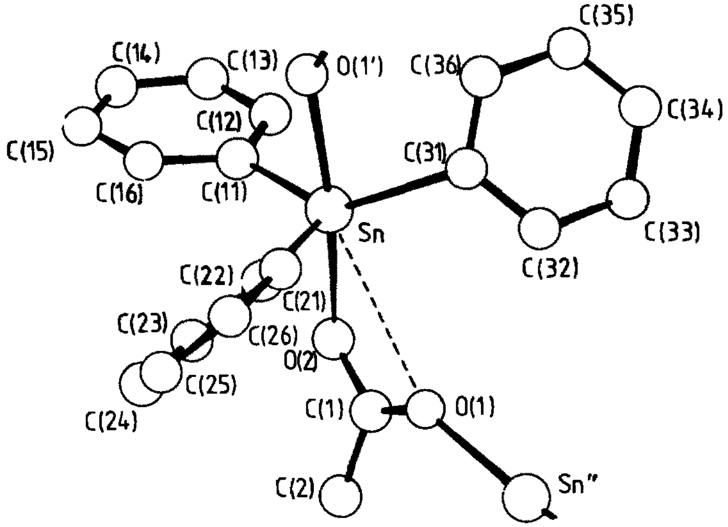

Fig. 1. The coordination about tin in $(C_6H_5)_3SnO_2CCH_3$ showing atomic labelling. The symmetry code for (′) and (″) atoms is given in Table 2.

together with atomic labelling is shown in Fig. 1. Lists of structure factors and thermal parameters are available on request from the authors (I.W.N.).

Discussion

The structure

The structure of triphenyltin acetate consists of polymeric chains in which essentially planar triorganotin moieties are bridged by carboxylate groups. The nature of this bridging is anisotropic, in which tin forms one short (Sn–O(2) 2.185(3) Å) and one relatively long (Sn–O(1′) 2.349(3) Å) bond to oxygen. The acetate groups are disposed in the usual *syn,anti*-fashion [8] with respect to pairs of tin atoms [9–18], which, coupled with a 2_1 axis coincident with the *b* axis of propagation, leads to a polymer which can alternatively be described as being of "flattened helical" or "stretched-S" construction (Fig. 2). This structure dominates the structural chemistry of organotin carboxylates (Table 3), and to which even the proposed monomers $(C_6H_{11})_3SnO_2CCH_3$ [16] and $(C_6H_{11})_3SnO_2CCF_3$ [17] have recently been reclassified [9]. Excluding bis(trimethyltin) malonate which is three dimensional by virtue of the bifunctional ligand [12], only three compounds deviate from this structure, triphenyltin *o*-(2-hydroxy-5-methylphenylazo)benzoate [9], trimethyltin glycinate [11] and tricyclohexyltin indole-3-acetate [19], and in each case the acyl oxygen is involved in hydrogen bonding. This feature appears enough to preclude polymer formation through carboxylate bridges, although chelation remains as a bonding option [9,19].

The two tin-oxygen bonds are comparable with the analogous bonds in related compounds (Table 3), although the covalent, ester Sn–O(2) bond (2.185(3) Å) lies towards the long end of the range found for such interactions (2.07–2.21 Å), while the formally coordinate, bridging Sn–O(1′) linkage (2.349(3) Å) is the shortest of its type yet reported.

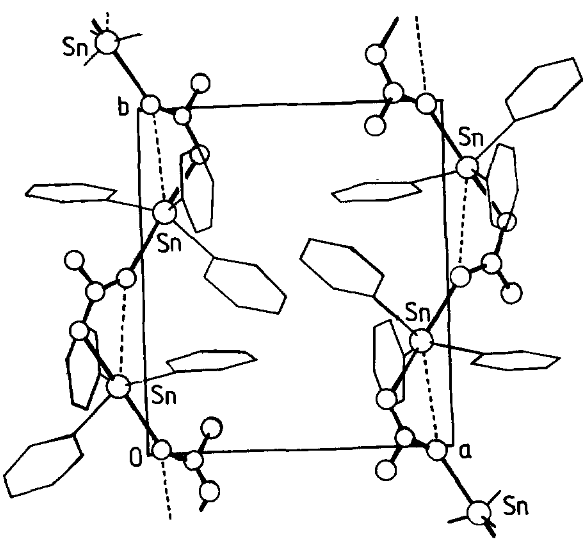

Fig. 2. A segment of the $(C_6H_5)_3SnO_2CCH_3$ polymer viewed perpendicular to the *a b* cell face.

The local geometry at tin is quite complex. Ostensibly, the coordination about the metal is a *trans*-R_3SnX_2 arrangement, in which the axial positions of the trigonal bipyramid are occupied by the more electronegative oxygens, while the α-carbons of the phenyl groups form the equatorial girdle (Fig. 1). There is, however, an additional weak Sn–O interaction arising from the acyl, bridging oxygen, which simultaneously chelates the tin from which the ligand emanates (Sn–O(1) 3.206(3) Å). Although long by comparison with both covalent or bridging coordinate Sn–O

TABLE 3

COLLECTED STRUCTURAL DATA FOR ORGANOTIN CARBOXYLATES[a,b]

Compound	Sn–O(2)	Sn–O(1′) inter	Sn–O(1) intra	C–Sn–C[c]	O(2)–C(1)–O(1)	Reference
$Ph_3SnO_2CCH_3$	2.185(3)	2.349(3)	3.206(3)	135.2(1)	1.263(5), 1.251(5)	This work
$Ph_3SnO_2CC_6H_4(N_2R)$-*o*[d]	2.070(5)	–	2.463(7)	117.0(2)[e]	1.296(8), 1.224(8)	[9]
$Me_3SnO_2CCH_3$	2.205(3)	2.391(4)	3.23	121.9(2)	1.269(5), 1.240(6)	[10]
$Me_3SnO_2CCF_3$	2.177(14)	2.458(15)	3.30	122.9(10)	1.28(2), 1.21(2)	[10]
$Me_3SnO_2CCH_2NH_2$	2.21(1)	–	3.23(3)	121.8(11)	1.34(3), 1.23(3)	[11]
$Me_3SnO_2CCH_2CO_2SnMe_3$	2.19(1)	2.46(2)	3.16	124.9	1.27(3), 1.22(3)	[12]
	2.17(1)	2.44(2)	3.12	123.6	1.28(3), 1.28(3)	
$Me_2(Cl)SnO_2CCH_3$	2.165(6)	2.392(7)	2.782(7)	140.9(6)	1.260(9), 1.262(10)	[13]
$Vin_3SnO_2CCCl_3$	2.17(2)	2.49(1)	3.30	124.8(5)	1.25(2), 1.21(2)	[14]
$Vin_3SnO_2C(Fer)$	2.12(1)	2.42(1)	3.21	127(1)	1.27(1), 1.21(2)	[15]
$Bz_3SnO_2CCH_3$	2.14(2)	2.65(2)	3.23(3)	123.8(14)	1.31(4), 1.21(4)	[16]
$Cyc_3SnO_2CCH_3$	2.12(3)	3.84	2.95(4)	113(1)	1.39(8), 1.25(9)	[17]
$Cyc_3SnO_2CCF_3$	2.08(4)	3.70	3.11	122	1.28(4), 1.20(5)	[18]

[a] Atomic numbering as in Fig. 1. [b] Abbreviations: Ph = C_6H_5, Me = CH_3, Vin = CH_2=CH, Bz = $C_6H_5CH_2$, Cyc = C_6H_{11}, Fer = $C_5H_4FeC_5H_5$. [c] C–Sn–C angle closest in proximity to O(1). [d] R = 2-hydroxy-5-methylphenyl. [e] *cis*-Ph_3SnX_2 geometry.

bonds, it is well within the sum of the two Van der Waals' radii (3.70 Å), and, moreover, severely distorts the equatorial C(21)–Sn–C(31) bond angle (135.2°) which is closest to the direction of O(1) approach to tin. Further evidence supporting the reality of this chelating interaction can be found from inspection of the two C–O distances within the ligand. Considering only the bridging role of the carboxylate, equality of the two C–O bonds will only arise when the two Sn–O bonds are equal i.e. bridging is isobidentate and the π-bond is symmetrically delocalised over the O–C–O framework. Such a situation generally does not occur in polymeric organotin caryboxylates, the bridging is anisobidentate and the majority of double bond character is localised in one C–O bond, manifesting itself in dissimilar C–O bond lengths (Table 3). In the title compound, however, despite a difference of ca. 0.164 Å in the two tin–oxygen bonds, the carbon-oxygen bonds are remarkably close (C(1)–O(1) 1.251(5); C(1)–O(2) 1.263(5) Å), a situation which can be rationalised in terms of additional electron withdrawal from the acyl C(1)–O(1) bond concomitant with formation of the chelating Sn–O(1) interaction. A similar argument has been used to rationalise the bifurcated Sn–S–Sn bonding in dimeric $\{Sn[S_2P(OPh)_2]_2\}_2$ [20].

The structure of triphenyltin acetate is thus best described in terms of a distorted *mer*-R_3SnX_3 geometry at tin, and represents the first crystallographically authenticated example of a six-coordinate triorganotin compound.

In related systems, $Cl(CH_3)_2SnO_2CCH_3$ has also been interpreted as being six-coordinate at tin [13] the coordination sphere about tin arising in exactly the manner described above for $(C_6H_5)_3SnO_2CCH_3$. Within the halotin acetate, the chelating Sn–O(1) bond is much stronger ([2.782(7) Å), manifesting itself in both a greater opening of the ∠C–Sn–C in the region of this interaction (140.9(6)°) and an equalising of C–O bond lengths (1.260(9), 1.262(10) Å) despite inequalities in the primary Sn–O bonds (2.165(6), 2.392(7) Å).

Considering the data for triorganotin carboxylates as a whole, it would appear that a coordination number of six at tin only occurs in compounds in which the Lewis acidity of the metal is enhanced by direct bonding to electron-withdrawing groups, chlorine in the case of $(CH_3)_2ClSnO_2CCH_3$ and three phenyl groups in the title compound. Trivinyltin derivatives might also be expected to show this tendancy, and a ∠C–Sn–C of 127(1)° in $(CH_2{=}CH)_3SnO_2C(C_5H_4FeC_5H_5)$ [15] suggests that this is possibly the case, although the phenomenon is clearly marginal.

Variable temperature Mössbauer study

Mössbauer data, embracing both the conventional isomer shift (*IS*) and quadrupole splitting (*QS*) parameters derived from the single temperature experiment, and more recent use of variable temperature studies to probe lattice dynamics [21, and ref. therein] have proved invaluable tools in the development of structural organotin chemistry. Key compounds such as triphenyltin acetate are often cited as reference points in the discussion of Mössbauer data of more esoteric compounds, and in the light of the current structure determination we present results of a variable temperature (78–145 K) study which highlight potential limitations in this area of Mössbauer methodology.

IS and *QS* values from the present study (1.28, 3.36 ± 0.03 mm s^{-1}, respectively) are in excellent agreement with earlier reports [6]. The magnitude of *QS* has generally been cited as evidence for a *trans*-R_3SnX_2 geometry at tin, largely by

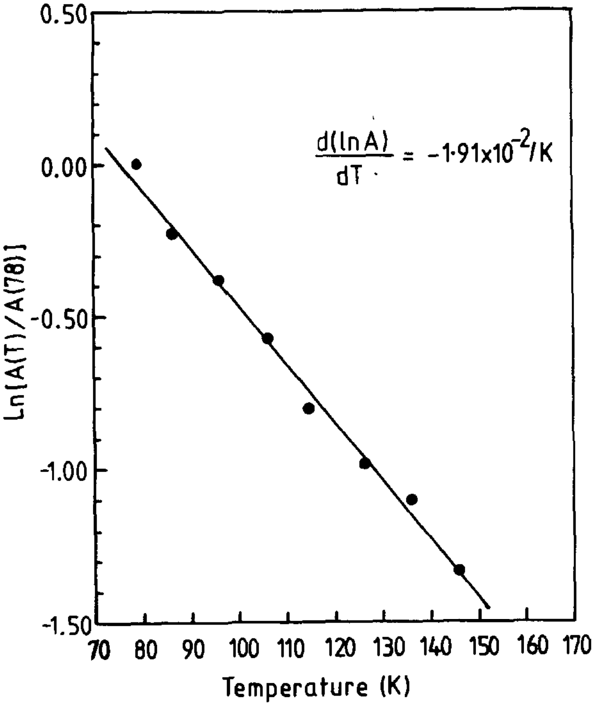

Fig. 3. Plot of the natural logarithm of the normalised area, ln [$A(T)/A(78)$] vs. temperature.

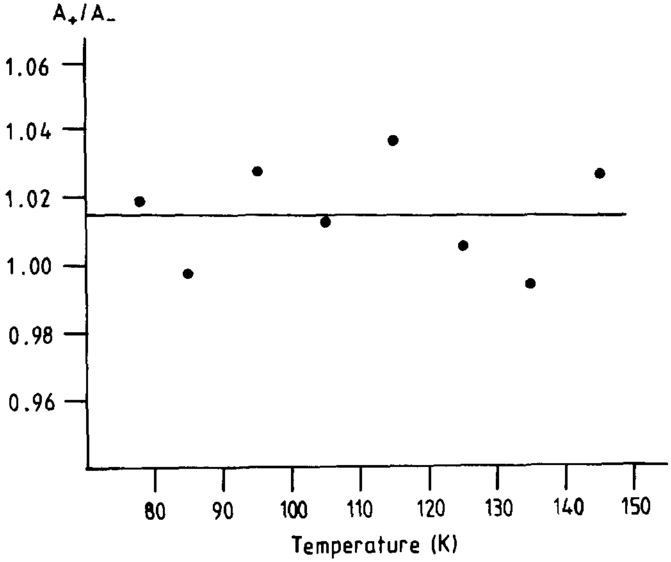

Fig. 4. Plot of the temperature dependence of the Mössbauer doublet spectrum line asymmetry. A_+ and A_- are the areas under the more positive and more negative velocity wings, respectively. The slope of the line is 1.28×10^{-5} K^{-1}.

comparison with predictions from point charge calculations [22], and in the light of the secondary nature of the bond which increases the coordination number at tin in this compound to six (Sn–O(1) 3.206(3) Å) this appears to be largely justified. We do, however, note that predicted *QS* values for *mer*-R_3SnX_3 structures are also ca. 3.50 mm^{-1} [23] and are equally applicable in this instance.

The lattice structure of organotins is reflected in *a*, the temperature dependance of the ^{119}Sn recoil-free-fraction $[f(T)]$ which in turn is related to the experimentally more accessible parameter $A(T)$, the area under the spectral envelope:

$$a = \frac{\mathrm{d}[f(T)]}{\mathrm{d}T} = \frac{\mathrm{d}[A(T)]}{\mathrm{d}T} \tag{1}$$

For a "thin absorber" ($N\sigma \leqslant 1$; N = number of absorber resonant atoms per cm^2, σ = resonant absorption cross-section of ^{119}Sn [24]), *a* can further be expressed as:

$$a = \frac{\mathrm{d}[\exp - \langle x_{\mathrm{iso}}(T) \rangle^2]}{\mathrm{dT}} \tag{2}$$

$$a = \frac{\mathrm{d}[\exp(-6E_{\mathrm{R}}T/k\theta_M)]}{\mathrm{d}T} \tag{3}$$

where $\langle x_{\mathrm{iso}}(T) \rangle^2$ is the mean-square amplitude of vibration of the Mössbauer atom at temperature T, E_{R} is the Mössbauer recoil energy, and θ_M a characteristic temperature equivalent to the Debye temperature. Plots of ln $A(T)$ vs. T should be linear and of slope *a*, and be characteristic of the tightness with which the Mössbauer atom is held in the lattice. For methyltins, values of $-a$ ca. 1.8×10^{-2} K^{-1} reflect non-interacting molecules, dropping to ca. 1.0×10^{-2} K^{-1} and lower for one- and higher-dimensional polymers, respectively [25]. Transfer of these systematics to phenyltin derivatives is broadly acceptable, although we have found that packing of the structured hydrocarbon groups in the latter case often mimic hydrogen bonding between methyltin compounds, based on comparable *a* values [26].

The plot of the ln $A(T)$ vs. T for the title compound is shown in Fig. 3. Although a non-thin sample was used to enable acceptable spectra to be accumulated within reasonable count times (ca. 12 h), no systemtic deviation from linearity in the plot is observed suggesting that lattice vibrational anharmonicity is also absent. The derived value of $-a$ is 1.91×10^{-2} K^{-1} (7 points; $r = -0.998$), which on the basis of the above systematics quite incorrectly predicts a monomeric rather than the observed 1-d polymeric lattice. Rationalisation of the data can be made in terms of the helical nature of the polymer, which has a two-fold effect on the distribution of atomic mass with respect to the direction of polymer propagation. Firstly, the tin atoms themselves do not lie along a single line, rather they are found alternatively either side of the 2_1 axis along *b*. Secondly, and more importantly, the direction in which the polymer is building at the tin is not along *b*, but approximately 60° to it based upon the general orientation of the O(1′)–Sn–O(2) unit. These factors combine to concentrate the bridging mass away from a line joining adjacent tin atoms, such that the space between tins is largely a void, and the bridging role of the carboxylate group is reduced to the long Sn–O(1) bond. The polymer thus has a "concertina-like" flexibility that confers a vibrational freedom upon the tin which more linear polymers do not. The motion of the tin thus becomes isotropic, a fact endorsed by the absence of any observable temperature dependent spectral line asymmetry

(Gol'danski–Karyagin effect; Fig. 4). This phenomenon is in sharp contrast to the related trimethyltin glycinate, in which tin atoms are O,N-bridged by the four atom backbone of the amino acid. The rigidity of this lattice is reflected in a value of $-a = 1.15 \times 10^{-2}$ K^{-1}, which in part arises from a network of hydrogen bonds approximately perpendicular to, and linking, adjacent polymer chains, but derives also a significant contribution from the polymer itself. This in turn is reflected in a sizeable Gol'danski–Karyagin effect arising from anisotropic vibrations of the tin, the majority of this motion occuring in the plane of the C_3Sn moiety and perpendicular to the O–Sn–N axis [11]. The structural variation which gives rise to these differences is that in the glycinate, the bridging O–C–C–N unit lies between tin atoms straddling the tin–tin vector to produce a linear extension of the chain, rather than the helical construction of the acetate which leaves largely a void between tin atoms.

We have found support for the above rationale in variable temperature Mössbauer studies of other polymeric systems. In particular, α-trimethyltin phenylphosphonate, $(CH_3)_3SnO_2P(C_6H_5)OH$, which is known to consist of helices held together into 2-d sheets by a network of strong hydrogen bonds [27], has $-a$ in the range $1.42–1.64 \times 10^{-2}$ K^{-1} [28], which on the basis of known systematics [25] merely reflects the contribution of the hydrogen bonds to lattice rigidity. As with triphenyltin acetate, incorporating the tin into a helical polymer does little (if anything) to inhibit vibrational motion of the tin, and it is only when helices are linked into sheets that such motion becomes anisotropic.

In conclusion, helical polymers are flexible enough to mimic non-interacting lattices with respect to the variable temperature Mössbauer experiment, and in instances where the bridging group is a multi-atom moiety, interpretation of data so derived must be tempered with caution.

Acknowledgements

We thank the National Board for Science and Technology (Ireland) for financial support (to K.C.M.), the S.E.R.C. (U.K.) for equipment grants (to I.W.N.) and the International Tin Research Institute for the supply of starting materials. One of us (T.G.P.) thanks the Department of Education (Ireland) for support in the form of a studentship.

References

1 A.G. Davies and P.J. Smith, Comprehensive Organometallic Chemistry, Pergamon Press 1982, p. 610.
2 M.H. Gitlitz, Adv. Chem. Ser., 157 (1976) 167.
3 J.S. Thayer and F.E. Brinkman, Adv. Organometal. Chem., 20 (1982) 313.
4 B. Sugavanam, Tin and Its Uses, 126 (1980) 4.
5 K.C. Molloy and T. Purcell, unpublished results.
6 B.F.E. Ford, B.V. Liengme and J.R. Sams, J. Organomet. Chem., 19 (1969) 53.
7 International Tables for X-ray Crystallography, Vol. IV, 1974, Table 2.2B, Kynoch Press, Birmingham (Great Britain).
8 L.R. Martin and H. Waterman, J. Chem. Soc., (1959) 1359.
9 P.G. Harrison, K. Lambert, T.J. King and B. Magee, J. Chem. Soc., Dalton Trans., (1983) 363.
10 H. Chih and B.R. Penfold., J. Cryst. Mol. Struct., 3 (1973) 285.
11 B.Y.K. Ho, K.C. Molloy, J.J. Zuckerman, F. Reidinger and J.J. Zuckerman, J. Organomet. Chem., 187 (1980) 213.

12 U. Schubert, J. Organomet. Chem., 155 (1978) 285.
13 D.W. Allen, I.W. Nowell, J.S. Brooks and R.W. Clarkson, J. Organomet. Chem., 219 (1981) 29.
14 S. Calogero, D.A. Clemente, V. Peruzzo and G. Tagliavino, J. Chem. Soc., Dalton Trans., (1979) 1172.
15 R. Granziani, V. Gasellato and G. Plazzogna, J. Organomet. Chem., 187 (1980) 381.
16 N.W. Alcock and R.E. Timms, J. Chem. Soc. A, (1968) 1873.
17 N.W. Alcock and R.E. Timms, J. Chem. Soc. A, (1968) 1876.
18 S. Calogero, P. Ganis, V. Peruzzo and G. Tagliavini, J. Organomet. Chem., 191 (1980) 381.
19 K.C. Molloy, T. Purcell, F.E. Hahn and H. Schumann, in preparation.
20 J.L. Lefferts, K.C. Molloy, M.B. Hossain, D. van der Helm and J.J. Zuckerman, Inorg. Chem., 21 (1982) 1410.
21 K.C. Molloy, M.P. Bigwood, R.H. Herber and J.J. Zuckerman, Inorg. Chem., 21 (1982) 3709.
22 B.F.E. Ford and J.R. Sams, J. Organometal. Chem., 31 (1971) 47.
23 N.W.G. Debye and J.J. Zuckerman, Develop. Appl. Spectrosc., 8 (1970) 267.
24 V.I. Gol'danski and E.F. Makarov, in V.I. Gol'danski and R.H. Herber (Eds.), Chemical Applications of Mössbauer Spectroscopy, Academic Press, 1968.
25 P.G. Harrison, R.C. Phillips and E.W. Thornton, J. Chem. Soc., Chem. Commun., (1977) 603.
26 K.C. Molloy and K. Quill, in preparation.
27 K.C. Molloy, M.B. Hossain, D. van der Helm, D. Cunningham and J.J. Zuckerman, Inorg. Chem., 20 (1981) 2402.
28 K.C. Molloy, K. Quill and D. Cunningham, unpublished results. The range of a values arises from non-linearity of the ln A vs. T plot.